European Polymer Journal 49 (2013) 2635–2644

Contents lists available at SciVerse ScienceDirect

European Polymer Journal

journal homepage: www.elsevier.com/locate/europolj

Macromolecular Nanotechnolgy

Incorporation of polybutadiene into waterborne polystyrene nanoparticles *via* miniemulsion polymerization

Ludmila I. Ronco [a], Roque J. Minari [a], Jorge R. Vega [a,b], Gregorio R. Meira [a], Luis M. Gugliotta [a,*]

[a] INTEC (Universidad Nacional del Litoral-CONICET), Güemes 3450, 3000 Santa Fe, Argentina
[b] Facultad Regional Santa Fe (Universidad Tecnológica Nacional), Lavaisse 610, 3000 Santa Fe, Argentina

ARTICLE INFO

Article history:
Received 22 February 2013
Received in revised form 30 May 2013
Accepted 5 June 2013
Available online 19 June 2013

Keywords:
Miniemulsion polymerization
Nanocomposites
Polystyrene
Polybutadiene rubber

ABSTRACT

The incorporation of polybutadiene in waterborne polystyrene nanoparticles by miniemulsion polymerization is expected to positively combine the properties of both materials, improving the impact resistance and toughness. The kinetics of the miniemulsion polymerization used to synthesize these hybrid nanomaterials and the effect of the reaction variables on the polymer microstructure and particle morphology were investigated. Both molecular microstructure and final particle morphology (core–shell, "salami" or three-phase type) depended on the nature of the employed polybutadiene based rubbers and initiators. The mechanisms responsible for these effects were discussed.

1. Introduction

In the production of engineering plastics, elastomeric particles are incorporated into brittle thermoplastic matrices to improve mechanical properties such as impact resistance and toughness. Thus, high-impact polystyrene (HIPS) is produced by incorporating polybutadiene (PB) into polystyrene (PS). To this effect, styrene (St) is polymerized in the presence of 5–10 wt% of PB in bulk (or quasi-bulk) processes that include a chemical initiator and reaction temperatures between 90 and 230 °C. The initial prepolymerization stage is carried out under stirring, and it ends at around 30% conversion. Then, an unstirred finishing stage is included to preserve the particle morphology generated at the end of the prepolymerization. In the continuous bulk processes, the final St conversion is limited to approximately 75% and the unreacted St is removed in a devolatilization stage [1,2]. The final HIPS may present different morphologies. In the "salami" morphology, the dispersed rubber particles exhibit diameters of 1 μm or larger, and are heterogeneous, with multiple vitreous PS occlusions. Smaller "core–shell" rubber particles containing single PS occlusions can also be produced. Alternatively, coils, mazes, shell, or capsule morphology could be obtained when partially replacing PB by St–butadiene (B) block copolymers [3,4].

Core/shell latex particles of PS and PB to be employed as impact modifiers have been produced in 2-stage emulsion polymerizations. Thus, Wei et al. [5] synthesized particles of a St/B block copolymer in 2 stages, with a miniemulsion polymerization of St by Reversible Addition–Fragmentation Chain Transfer (RAFT) followed by a PS seeded RAFT emulsion polymerization of B. They observed that particle morphology depends on the composition of the PS-co-PB segment. Gao et al. [6] investigated the mechanical properties of modified PS obtained by mixing PS with core–shell PB-g-PS rubber particles synthesized *via* emulsion polymerization of styrene in the presence of a polybutadiene latex. A redox water-soluble initiator produced small PS microphases inside the rubber core, yielding a low toughness and low impact strength material. However, both mechanical properties were improved when employing the oil-soluble initiator 1,2-azobisisobutyronitrile, due to the larger PS occlusions generated in the rubber core. Also, this type of core–shell particles of PB-g-PS were introduced

* Corresponding author. Tel.: +54 342 4511546; fax: +54 342 4511079.
E-mail address: lgug@intec.unl.edu.ar (L.M. Gugliotta).

0014-3057/$ - see front matter © 2013 Elsevier Ltd. All rights reserved.
http://dx.doi.org/10.1016/j.eurpolymj.2013.06.011

into commercial HIPS to improve the mechanical properties of the resulting composite [7].

Miniemulsion (ME) polymerization represents an alternative for the synthesis of hybrid latexes; and enables the incorporation of a hydrophobic component into the polymer particles in a single step process, without requiring its diffusion through the aqueous phase. Many publications have been focused on the production of waterborne coatings and adhesives by ME polymerization, such as polyurethane-acrylic hybrid nanoparticles [8,9], hybrid latex particles of acrylic and tackifying resins [10], and acrylic/alkyd "solvent-free" coatings [11]. Thus, ME polymerization could enable the production of nanostructured particles with potential applications as reinforced materials, by direct incorporation of B-based rubbers into PS nanoparticles; with the advantage of reducing the mixing and heat transfer problems compared to an equivalent bulk (or quasi-bulk) process.

Besides the article by Jia et al. [12] which employs small quantities of a low molecular-weight PB (liquid PB) with the aim of co-stabilizing the ME polymerization of St, Jeong et al. [13] is so far the single publication that describes the synthesis of hybrid composite latex by ME polymerization, with incorporation of a B-based rubber into PS particles. The base rubber was a SBS triblock copolymer (Kraton®), and it was added in a 20/80 rubber/St weight ratio. The miniemulsions were prepared with a Manton–Gaulin high pressure homogenizer followed by a membrane filtration to eliminate the larger ME droplets. When observing the rubber particles by transmission electron microscopy (TEM) after their fractionation by density gradient centrifugation, different SBS contents were seen between the larger and smaller particles, as a consequence of the faster nucleation of smaller particles with respect to the bigger ones. Only cellular morphologies were observed, and the molecular characteristics of the polymers was not determined [13].

In the present work, the ME polymerization of St in the presence of PB or styrene–butadiene rubber (SBR) is investigated, with the aim of synthesizing waterborne PS-rubber nanocomposites with different molecular microstructures and particle morphologies, able to be applied as a nanostructured engineering plastic. The polymerization kinetics, molecular microstructure, and particle morphology were followed along several reactions, with different combinations of temperature, rubber type and content, and initiation systems.

2. Experimental

2.1. Materials

Demineralized water was used throughout the work. The following reagents were employed as received: potassium persulfate (KPS) from Mallinckrodt (99% purity) was the water soluble initiator; benzoyl peroxide (BPO) from B.D.H. (wet, with 30% water) was the organic soluble initiator; and tert-butyl hydroperoxide/ascorbic acid (TBHP/AA), Aldrich/Cicarelli (molar ratio 2/1) was the water soluble redox initiation system. In addition, hexadecane (HD) from Merck ($\geqslant$99% purity) was the costabilizer; sodium lauryl sulphate (SLS) from Cicarelli (95% purity) was the surfactant; and hydroquinone (HQ) from Fluka AG (>99% purity) was the polymerization inhibitor. Styrene was washed with an aqueous solution of potassium hydroxide (to remove polymerization inhibitors), and then with demineralized water until reaching the pH of the washing water. Three different rubbers were employed (see characteristics in Table 1): a PB (Buna CB 55 GPT) from Lanxess; and two SBR from Petrobras Argentina: a commercial Arpol 1502 sample of a higher molecular weight (SBR_H), and a non-commercial sample of lower molecular weight (SBR_L). A set of 9 (Shodex) narrow PS standards in the range 10^3–10^6 g/mol was used to calibrate the size exclusion chromatograph. Tetrahydrofuran (HPLC Solvent, J.T. Baker) was the eluent of the size exclusion chromatography SEC runs. Methyl–ethyl ketone (MEK, Anedra, 99% purity) was employed as a selective solvent for determining the degree of grafting.

2.2. Miniemulsification

All the miniemulsions contained: (a) 20–30% wt of solids; (b) a variable rubber content; (c) 2–2.5% wbop (weight based on organic phase) of surfactant; (d) 4% wbm (weight based on monomer) of HD; and (e) a 0.024 M in aqueous phase of $NaHCO_3$. The rubber was dissolved in the organic phase for 12 h before the miniemulsification. To produce the ME, the organic and aqueous phases were first strongly mixed by magnetic stirring during 15 min., and the resulting preemulsion was sonified in a Sonics VC 750 (power 750 watts) during 25 min. at 100% of amplitude, and with cycles of 20 s on and 5 s off.

2.3. Polymerizations

Polymerizations were carried out in a 0.3 L batch glass reactor equipped with a reflux condenser, a stirrer, a sampling device, and a nitrogen inlet. The reaction temperature (70–90 °C) was adjusted by manipulating the reactor jacket temperature with a controlled water bath. The ME was loaded into the reactor, and the system was kept under stirring and with nitrogen bubbling until the sought reaction temperature was reached. The BPO initiator was dissolved in the organic phase prior to preparation of the ME. The KPS initiator was dissolved in water and injected into the reactor as a shot. In the experiments with TBHP/AA, 20% of these reactants were loaded at the start of the polymerization, and the remaining 80% were fed during 45 min. in separate streams and at constant flow rates. The total polymerization times were 2 h for the reactions with KPS and TBHP/AA, and 3 h for the reactions with BPO.

Table 1
Base characteristics of the three base rubbers.

Rubber	B content (weight%)	$\bar{M}_n \times 10^{-3}$ (g mol^{-1})	$\bar{M}_w \times 10^{-3}$ (g mol^{-1})
PB	100	275.5	445.0
SBR_H	76.5	105.0	305.0
SBR_L	76.5	25.3	91.3

The TBHP/AA system and KPS generate radicals in the water phase, while BPO generates radicals in the organic phase. Terbutoxy radicals from TBHP/AA are highly hydrophobic, and can directly enter into the organic phases. In contrast, SO_4^- radicals from KPS must polymerize in the water phase and gain hydrophobicity, prior to entering into the organic phase.

2.4. Characterization

The ME stability was measured in a Turbiscan TMA2000, by determining the profile of backscattered light intensity along a vertical tube every 5 min., and during 4 h.

The following was measured onto samples withdrawn along the reactions: (i) monomer conversion (x), by gravimetry and (ii) average droplets diameter ($\bar{d}_d$), particles diameter ($\bar{d}_p$), and intensity-based particle size distributions by dynamic light scattering (DLS) at a detection angle of 90°, in a Brookhaven BI-9000 AT photometer. To avoid destabilization and monomer lost in droplets and particles, the samples were diluted prior to the DLS measurements with a water solution saturated with SLS and St. In addition, the mass of final latex coagulum was measured after filtration with a 85 μm nylon mesh.

The coagulum composition was determined by ^{1}H NMR, in a Brüker Avance 300 spectrometer at 300.14 MHz. The sample was swollen with chloroform-D_6. Fig. 1 presents a typical spectrum. The number of St and B units per proton (S_H and B_H, respectively) were calculated as follows [14]:

$$S_H = \frac{A_{\delta=7.5-6.2}}{5} \quad (1)$$

$$B_H = \frac{A_{\delta=5.4} - 0.5A_{\delta=4.9}}{2} + \frac{A_{\delta=4.9}}{2} \quad (2)$$

where $A_{\delta=7.5-6.2}$ is the total area of aromatic St protons; $A_{\delta=5.4}$ is the area of the olefinic protons in the *cis* and *trans* *B* units + one methine proton of the olefinic protons of the vinyl sequence; and $A_{\delta=4.9}$ is the signal area of the olefin CH_2 in the vinyl-1,2 *B* units.

Then, the following expressions were used to calculate the weight% of B-based rubber in the coagulum ($Rubber_{coag}$):

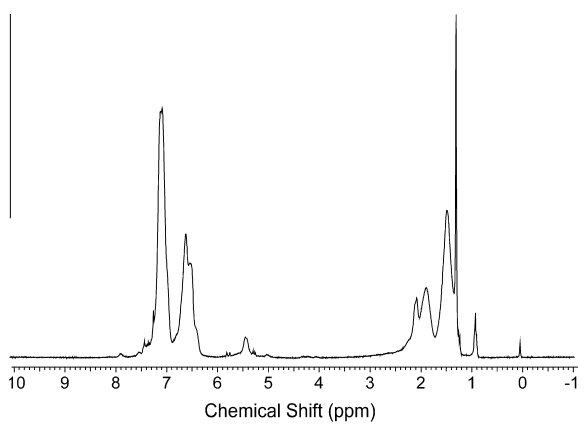

Fig. 1. ^{1}H NMR spectrum of a coagulum sample swollen with chloroform-D6.

With PB:

$$Rubber_{Coag} = \frac{B_H \times 54.09\,gmol^{-1}}{B_H \times 54.09\,gmol^{-1} + S_H \times 104.15\,gmol^{-1}} \times 100 \quad (3)$$

With SBR:

$$Rubber_{coag} = \frac{B_H \times 54.09\,gmol^{-1} + (\frac{1-0.765}{0.765})B_H \times 54.09\,gmol^{-1}}{B_H \times 54.09\,gmol^{-1} + S_H \times 104.15\,gmol^{-1}} \times 100 \quad (4)$$

The gel content was determined by Soxhlet extraction under THF reflux of vacuum-dried polymer samples over a period of 24 h. The molecular weight distribution (MWD) and averages ($\bar{M}_n$ and $\bar{M}_w$) of the final samples were determined by SEC. The measurements were carried out with a Waters 1515 chromatograph fitted with a Styragel HR 5E column from Waters Corp., of nominal fractionation range of 10^3–10^7 g/mol; and two on-line detectors: a differential refractometer (DR, Waters 2414) and a UV photometer at 254 nm (Waters 440).

The grafting efficiency (E_g) is defined as the mass of grafted St with respect to the total mass of polymerized St. The mass of grafted PS onto the original rubbers (PB or SBR) was determined by solvent extraction, by dissolution of the free PS in MEK; while the B-based components (including the grafted polymer) remained insoluble [15]. To this effect, 0.3 g of the dry final sample was first dispersed in 10 mL of MEK and shaken for 12 h. Then, the mixture was centrifuged at 3000 rpm during 2 h. The clear supernatant containing the dissolved PS was isolated, and the remaining polymer was precipitated with methanol. The process was repeated onto the undissolved fraction, until absence of free PS in the supernatant. The remaining insoluble was dried and the percentage of grafted PS was calculated from:

$$E_g = \frac{\text{Wt of insoluble material} - \text{initial wt of rubber in the sample}}{\text{Total wt of PS in the sample}} \times 100 \quad (5)$$

Particle morphology was determined by TEM, in a JEOL 100 CX (100 kV). Samples of diluted latex were stained in liquid phase with a 2 wt% aqueous solution of osmium tetroxide for 2 h. OsO_4 reacts with the B double bonds, and shows a dark rubber phase. Then, a drop of the stained and diluted latex was placed on copper grids covered with polyvinyl formal (Formvar® by Fluka), and dried at room temperature. The micrographs were taken at different magnifications, depending on particle size.

3. Results

3.1. Miniemulsions

Table 2 summarizes the recipes, reaction conditions, and global results of the 17 experiments. Except for Exps. 5 and 9 (of solids content 30%), and Exp. 17 (of SLS concentration 2.5% wbop), in all the other experiments the solids content was 20%, and the SLS concentration was 2% wbop.

Table 2
Recipes and final results of the ME experiments.

Exp.	Rubber (% wbop)	Initiator (% wbm)	Temperature (°C)	$\bar{d}_d$ (nm)	x[a] (%)	$\bar{d}_p$ (nm)	N_p/N_d [b]	Coagulum (%)[c]
1	SBR_H (1)	KPS (0.75)	70	167	92	106	3.9	<0.01
2	SBR_H (5)	KPS (0.75)	70	245	89	110	11.2	0.04
3	SBR_L (1)	KPS (0.75)	70	114	93	101	1.4	0.04
4	SBR_L (5)	KPS (0.75)	70	201	92	106	6.8	<0.01
5[d]	PB (5)	KPS (0.75)	70	331	96	102	34.2	Absence
6	PB (5)	KPS (1.5)	70	229	94	108	9.5	0.08
7	SBR_H (1)	TBHP/AA (1.5)	70	182	92	108	4.7	<0.01
8	SBR_L (5)	TBHP/AA (1.5)	70	216	93	108	7.9	<0.01
9[d]	PB (5)	TBHP/AA (1.5)	70	362	95	100	47.4	0.1
10	PB (5)	TBHP/AA (1.5)	70	255	90	97	18.0	<0.01
11	SBR_L (5)	BPO (0.5)	70	208	5.7 (9)	222	0.82	Absence
12	SBR_L (5)	BPO (2.1)	70	205	35 (52)	189	1.3	Absence
13	SBR_L (5)	BPO (2.1)	80	208	75 (95)	189	1.3	Absence
14	SBR_L (10)	BPO (2.1)	80	245	60 (80)	204	1.7	1.8
15	PB (5)	BPO (2.1)	80	282	67 (84)	243	1.6	0.8
16	PB (5)	BPO (2.1)	90	287	85 (85)	225	2.0	2.2
17[e]	PB (5)	BPO (2.1)	90	254	82 (84)	219	1.6	1.0

[a] Conversion at 2 h of polymerization; in the reactions with BPO, x at 3 h is also reported in parentheses.
[b] Ratio of final particles number to droplets number.
[c] Weight based on total latex.
[d] 30% Solids content.
[e] 2.5% wbop of SLS.

According to the backscattering profiles measured with the Turbiscan analyzer during 4 h, all the ME remained stable at room temperature. Under identical miniemulsification conditions, it is expected that an increase in the rubber content and/or in its molecular weight will increase the organic phase viscosity, and therefore the ME droplets size (see Table 2). The droplet diameters resulted smaller than 200 nm only in the experiments containing 1% of rubber (i.e., in Exps. 1, 3, and 7). In all the other experiments, $\bar{d}_d > 200$ nm. The final $\bar{d}_d$ results from an interplay between coalescence and droplets break-up. For otherwise identical homogenization conditions, coalescence is governed by the emulsifier content, while the droplets break-up mainly depends on the viscosity of the organic phase. An additional ME was prepared with solids content 20% and 5% wbop of PB, but with a higher SLS concentration (3% wbop); yielding: $\bar{d}_d = 250$ nm (a similar value to those of Exps. 6 and 10). This suggests that the miniemulsification process is mainly controlled by the organic phase viscosity that restricts the droplets break-up.

3.2. Kinetics

Independently of the rubber type and its concentration, after 2 h of reaction time, the final conversions observed with KPS and TBHP/AA were around 90% (i.e., higher than those with BPO). In addition, the water-soluble initiators yielded final $\bar{d}_p$ values of around 100 nm, while the larger $\bar{d}_p$ values were observed with BPO. Fig. 2 shows the evolution of x and $\bar{d}_p$ for the polymerization of St in the presence of the different rubbers and with KPS as initiator. In the 4 reactions with SBR (Exps. 1–4), conversion was little affected by the concentration or $\bar{M}_w$ of the employed SBR (Fig. 2a, Table 2). Also, $\bar{d}_p$ decreases along these polymerizations from the initial $\bar{d}_d$ (Fig. 2b). This suggests a significant secondary nucleation by micellar or homogeneous mechanism, promoted by hydrophilic radicals from water-soluble initiators (like KPS) [8,11]. As expected, the organic phase viscosity was reduced when decreasing either the amount of SBR or its $\bar{M}_w$. This in turn reduced $\bar{d}_d$, increased the total droplets area, and increased the probability of droplet nucleation (Exps. 1 and 3, Table 2). The highest droplet nucleation efficiency ($N_p/N_d \approx 1$) with an almost constant $\bar{d}_p$, was observed in Exp. 3 with 1% wbop of SBR_L (Fig. 2b). When using 5% wbop of PB, polymerization rate was not affected by the solids content increment (Fig. 2c). The high N_p/N_d values and the decreasing $\bar{d}_p$ along the polymerization (Fig. 2c) of Exps. 5 and 6, suggest that most of the particles were formed by secondary nucleation. In Exp. 5, the higher values of $\bar{d}_d$ and solids content (30%) promoted the unwanted secondary nucleation.

Fig. 3 compares the evolutions of x and $\bar{d}_p$ in equivalent reactions with TBHP/AA and KPS. The redox initiator exhibits an increased generation of radicals and an increased polymerization rate (Fig. 3a and c). However, the N_p/N_d ratio is not improved with respect to the KPS case (Table 2), due again to a significant secondary nucleation.

Coagulum was practically negligible in the experiments with KPS and TBHP/AA. Possibly, the formation of a small coagulum is promoted by phase separation of non-nucleated droplets, due to St migration toward the particles generated by secondary nucleation. The SEC analysis (by DR + UV at 254 nm) of the coagulum in Exp. 6 suggests that it mainly consists of PB (at 254 nm, the PB absorbance is negligible).

Secondary nucleation is little promoted by the oil-soluble initiator BPO (water solubility: 3×10^{-4} g/100 g) [16]. This is because radicals are formed inside the droplets, and their water solubility is limited. At 70 °C, the decomposition rate constant of BPO ($k_{d(BPO)} = 1.31 \times 10^{-5}$ s^{-1}) [17] is similar to that of KPS ($k_{d(KPS)} = 2.17 \times 10^{-5}$ s^{-1}) [18]. However, a low monomer conversion was obtained with BPO at 0.5% wbm and 70 °C (Exp. 11). This could be

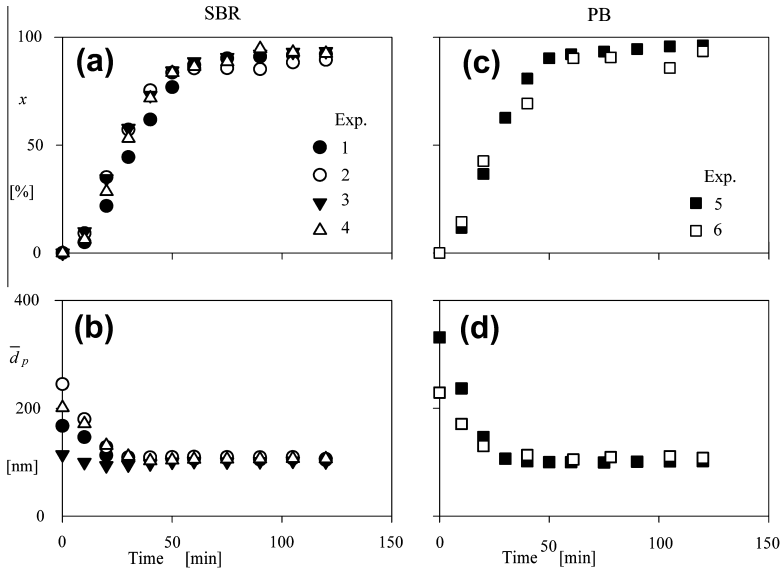

Fig. 2. St ME polymerization with KPS as initiator and in the presence of SBR (a and b) or PB (c and d). Evolution of conversion (a and c), and average particle diameter (b and d).

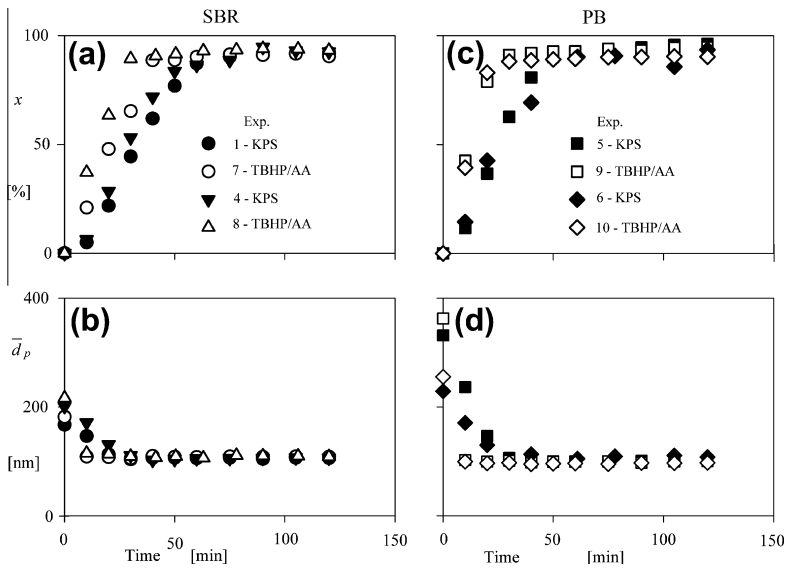

Fig. 3. St ME polymerization in the presence of SBR (a and b), or PB (c and d) for different initiation systems (KPS or TBHP/AA). Evolution of conversion (a and c) and average particle diameter (b and d).

due to the lower efficiency of primary radicals produced inside the droplets and polymer particles, compared to those generated in the aqueous phase. A large fraction of BPO radicals are restricted to a small volume, thus enhancing bimolecular termination [19]. For this reason, the experiments with BPO involved higher initiator concentrations, higher temperatures (80, 90 °C), and extended polymerization times (3 h).

Fig. 4 shows the evolution of x, $\bar{d}_p$, and N_p/N_d in the polymerizations with BPO. Exps 12–14 contained between 5% and 10% wbm of SBR_L, and Exps. 15–17 contained 5% wbm of PB. In all these experiments, droplet nucleation was predominant, as suggested by their N_p/N_d ratios close to unity. Note that the polymerization rate and the final monomer conversion obtained with 2.1% wbm of BPO is very low at 70 °C (Exp. 12), while the final x at 80 °C is 95% after 3 h of reaction (Exp. 13). The rate of polymerization was reduced when increasing the SBR_L content to 10% wbop (Exp. 14, Fig. 4a). This is because the number of droplets was slightly reduced, due to the increased organic phase viscosity. Also, a significant amount of coagulum was collected when increasing SBR_L from 5% to 10% wbm (Exp. 14). Compared to the experiments with KPS, BPO produced a lower polymerization rate, mainly due to its re-

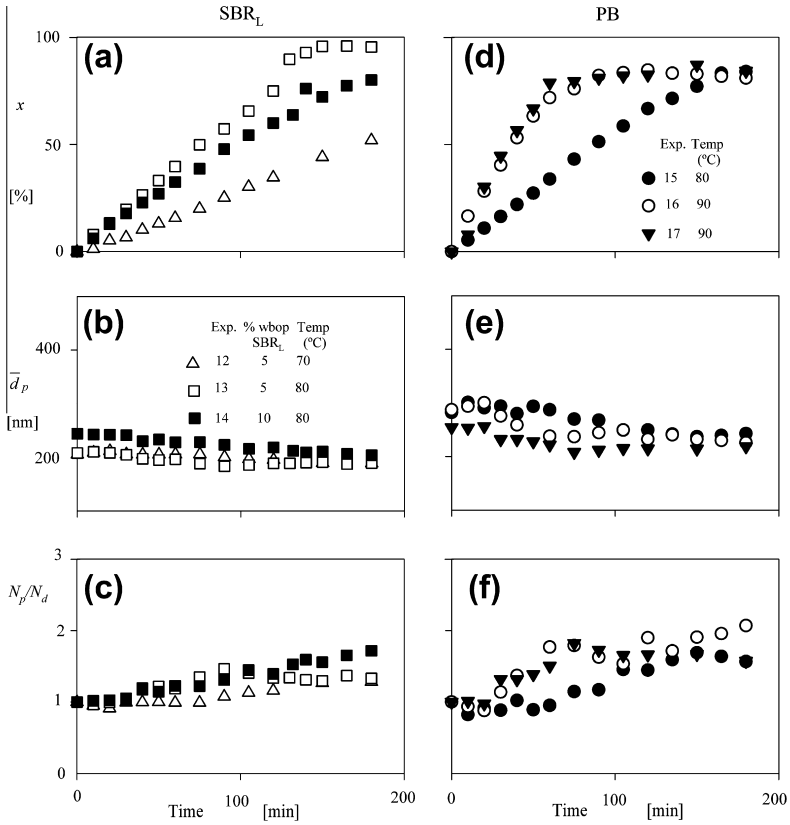

Fig. 4. St ME polymerization in the presence of SBR_L (a–c), or PB (d–f) with BPO as initiator. Evolution of conversion (a and d), average particle diameter (b and e), and N_p/N_d ratio (c and f).

duced initiation efficiency and lower N_p (since most of the particles were produced by droplet nucleation).

In the experiments with PB, the increase in temperature from 80 to 90 °C (Fig. 4d–f) increased the polymerization rate and the amount of coagulum, but did not affect the final conversion. An SLS content of 2.5% wbop (Exp. 17) reduced the coagulum with respect to Exp. 16 (with 2% wbop of SLS), without significant variation in polymerization rate.

In spite of the significant droplet nucleation with 2.1% wbm of BPO, $\bar{d}_p$ slightly decreased along the polymerization. This may be caused by a secondary nucleation mechanism. But since BPO exhibits low water solubility, relatively few particles are expected to be formed in such way. In addition, in the experiments with high coagulum contents (Exp. 14–17), $\bar{d}_p$ decreases along the polymerization, with N_p/N_d values between 1.5 and 2. This could be due to the coalescence of the bigger and more unstable particles which lead to coagulum (precipitated and/or trapped in the reactor inserts), resulting in final latexes of smaller particles. Table 3 summaries the weight% of rubber contained in the coagulum ($Rubber_{coag}$) for the experiments with BPO (Exps. 14–17), as measured by ^1H NMR. The $Rubber_{coag}$ are low and close to the original rubber compositions (Table 2), thus indicating formation of coagulum from nucleated droplets. Fig. 5 shows intensity-based size distributions for the ME droplets and polymer particles, as determined by numerical inversion of the

Table 3
Coagulum composition by ^1H NMR for experiments with BPO.

Exp.	$Rubber_{Coag}$ (%)
14	7.5
15	3.2
16	5.1
17	4.0

DLS autocorrelation functions [20]. After disappearance of the larger nucleated droplets by coagulation, the particle size distribution becomes narrower, and with a lower $\bar{d}_p$. This effect is more pronounced in Exps. 14 and 16, where the highest coagulum contents were observed (Fig. 5b and c). A low deviation is observed between the droplet and particle size distributions in Fig. 5a for Exp. 13, where coagulum is negligible.

3.3. Polymer structure

Table 4 presents the gel content, grafting efficiency, and average molecular weights of the free PS (isolated by solvent extraction). Important differences are observed in E_g, $\bar{M}_n$, $\bar{M}_w$, and gel%, according to the employed initiator (KPS, TBHP/AA or BPO). Since the ME polymerization of St does not produce gel and that the employed B-based rubbers do not contain an appreciable insoluble fraction (after

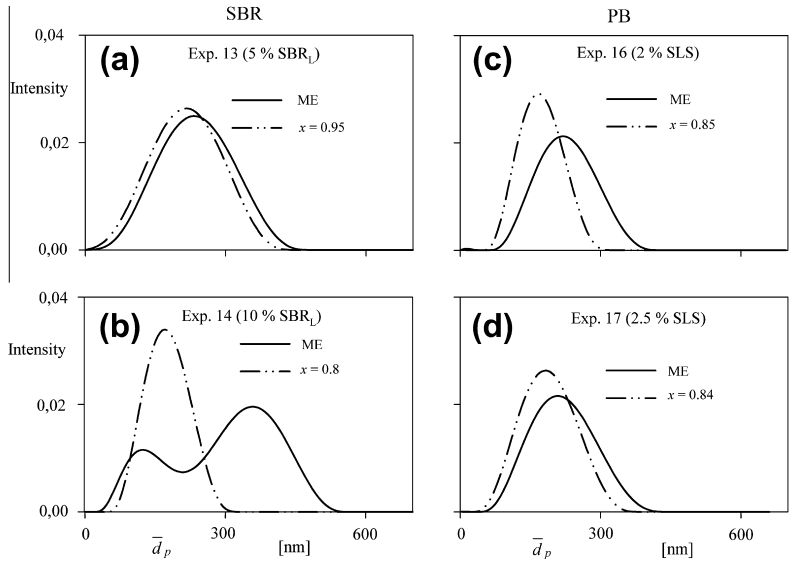

Fig. 5. Intensity-based droplet and particle size distributions for the experiments with BPO as initiator and SBR (a and b) or PB (c and d) as preformed polymer. Results for the initial miniemulsions and for the final latexes.

Table 4
Gel content and grafting efficiency of the final latex, and average molecular weights of the free PS.

Exp.	Rubber (% wbop)	Initiator (% wbm)	Gel (%)	E_g (%)	$\bar{M}_{nPS}$ (g mol^{-1})	$\bar{M}_{w\ PS}$ (g mol^{-1})
2	SBR$_H$ (5)	KPS (0.75)	3.2	4.7	208,000	2,218,000
4	SBR$_L$ (5)	KPS (0.75)	2.2	3.1	214,000	1,843,000
5	PB (5)	KPS (0.75)	2.3	7.5	236,000	1,959,000
6	PB (5)	KPS (1.5)	2.2	3.4	141,000	2,164,000
8	SBR$_L$ (5)	TBHP/AA (1.5)	1.1	4.4	42,000	285,000
9	PB (5)	TBHP/AA (1.5)	3.0	8.5	40,000	224,000
10	PB (5)	TBHP/AA (1.5)	3.3	5.6	27,000	278,000
13	SBR$_L$ (5)	BPO (2.1)	8.8	5.5	18,000	147,000
14	SBR$_L$ (10)	BPO (2.1)	21.0	8.9	11,000	78,000
15	PB (5)	BPO (2.1)	17.0	13.7	13,000	80,000
16	PB (5)	BPO (2.1)	21.7	14.4	11,000	66,000
17	PB (5)	BPO (2.1)	17.8	14.0	11,000	62,000

a THF extraction), then the gel isolated after ME polymerization corresponds to insoluble grafted copolymer.

Compared to the water soluble initiators, BPO produces higher gel contents and grafting efficiencies. Grafting mainly occurs by abstraction of allylic hydrogens from the PB chains [21–23]. Compared to styryl radicals, oxygen-centered radicals (as produced by decomposition of BPO) are more able to abstract hydrogen from PB [24]. In addition, at 90 °C the chain transfer capacity of the initiator radicals is 1400-fold higher than styryl radicals [25]. KPS and TBHP/AA also give oxygen-centered radicals, but these radicals are produced in the water phase. Sulfate radicals generated by decomposition of KPS are rather hydrophilic, and must polymerize in the water phase prior to entering into the organic phases. Styryl radicals incoming into the rubber particles from the water phase, induce less grafting and gel than primary BPO radicals. The hydrophobic tert-butoxyl radicals produced from TBHP/AA can directly enter into the organic phases without polymerizing in water phase. However, their lower efficiency for droplet nucleation (see high N_p/N_d in Table 2) importantly reduces the probability of grafting, as shown in Table 4.

Consider now the average molecular weights of the free PS. The highest values were obtained with the water soluble KPS initiator, and the lowest with BPO. The $\bar{M}_w$ values obtained with KPS are similar to those produced in an emulsion polymerization of St with molecular weight control by chain transfer to the monomer, and particle size in the range 90–130 nm [26]. However, the low values of $\bar{M}_n$ could be caused by a greater contribution of termination reactions that can take place in bigger particles nucleated from ME droplets and with higher radical concentration (Fig. 6). The oil-soluble tert-butoxyl radicals produce lower free-PS molecular weights with respect to those obtained with KPS. Finally, BPO was included in high concentrations and yields a pseudo-bulk system, with large particles of $\bar{d}_p > 200$ nm. This induces an increased termination that reduces the PS molecular weights.

3.4. Particle morphology

Fig. 6 shows the TEM image of the particles obtained in Exp. 5 with KPS and PB, which also includes a zoom of a hybrid particle. Most of the particles are homogeneous

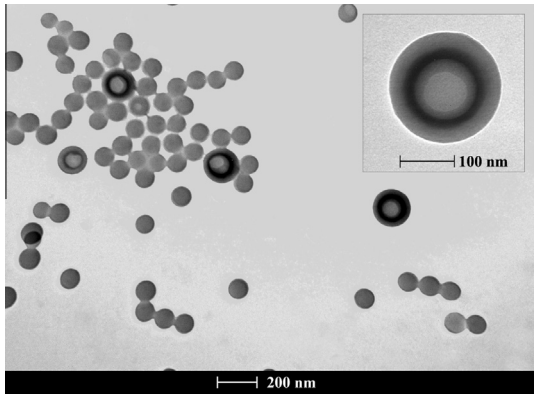

Fig. 6. TEM of the hybrid particles in the final latex of Exp. 5 with 5% wbop of PB and KPS as initiator.

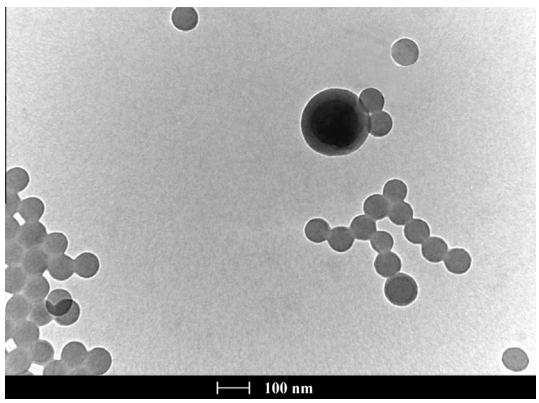

Fig. 7. TEM of the hybrid particles in the final latex of Exp. 10 with 5% wbop of PB and TBHP/AA as initiator.

without internal morphology, and were formed by secondary nucleation. In addition, some of the particles present a 3-phase internal morphology, with a PS shell, an intermediate PB-enriched phase, and a partially hollow PS core. In Exp. 10 with TBHP/AA, most of the particles were also formed by secondary nucleation, generating homogeneous PS particles (Fig. 7). However, some of the particles that mainly contain PB present phase separation and core–shell morphology. Possibly, the bigger particles formed by droplet nucleation lost most of their monomer by diffusion into the smaller growing particles. Due to their low St content and grafting efficiency (Table 4), these particles do not exhibit a complex morphology. Finally, in the experiments with PB and BPO, larger occluded rubber particles with multiple PS occlusions are observed (Fig. 8). In contrast, the smaller particles are more homogeneous because they mainly consist of PS. However, in a closer examination, most of the smaller particles exhibit a thin black ring of a PB-rich phase. Similar difference in rubber content between large and small particles has been previously observed [13].

Fig. 9 shows the TEM image of Exp. 14 with 10% wbop of SBR_L and BPO as initiator. In this case, the greater compatibility of SBR towards PS generates a 2-phase morphology,

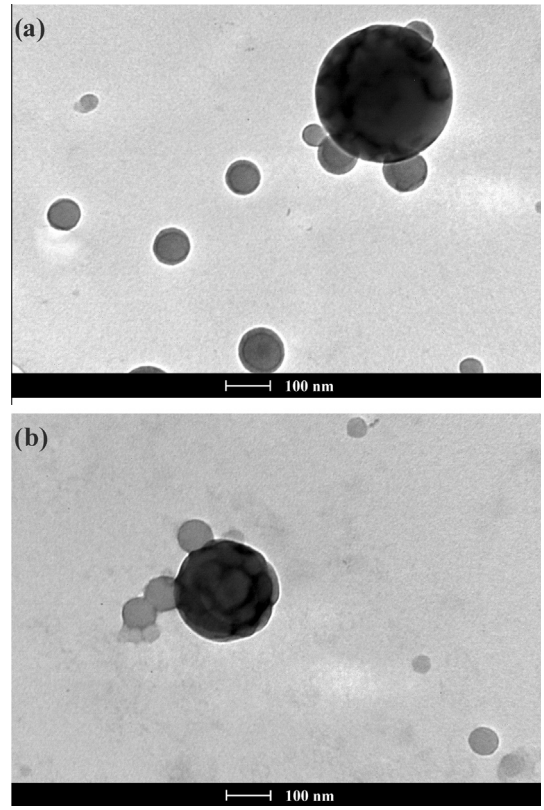

Fig. 8. TEM of the hybrid particles in the final latex of Exps. 16 (a) and 17 (b) with 5% wbop of PB and BPO as initiator.

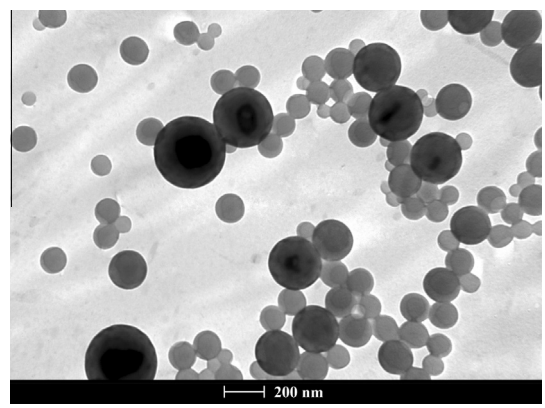

Fig. 9. TEM of hybrid particles in the final latex of Exp. 14 with 10% wbop of SBR_L and BPO as initiator.

with a SBR-rich core and a PS-rich shell. Even though not shown, no appreciable phase separation was observed in the particles of Exps. 1–4, 7–8, and 11–13 (with low SBR contents of 1–5% wbm).

Phase separation was only observed in particles produced by droplet nucleation. Thus, consider the morphology development in particles produced by droplet nucleation. The polymerization starts with homogeneous

droplets containing a St solution of dissolved rubber. Phase separation in nanoparticles is expected to occur at a low St conversion (between 0.5% and 2%), and thereafter the morphology consists of PS-rich nanodroplets dispersed in a PB-rich phase. The PB-g-PS chains in principle stabilize the PS-rich/PB-rich interface and promote development of the final morphology. An early production of graft copolymer would stabilize the PS droplets and prevent their coagulation [21]. In contrast, with a low grafting efficiency, the PS droplets that remain trapped in the PB-rich phase would tend to coagulate into single occlusions.

The low degree of grafting obtained with KPS promotes coagulation of the PS-rich nanodroplets, yielding a single PS-rich core, an inner PB-rich shell, and a PS shell. The monomer contained in the PS-rich core is inaccessible to the propagating radicals that enter from the aqueous phase [27], since they should diffuse through the 2 outer layers. Then, during the TEM preparation, the unreacted St contained in the PS cores is volatilized prior to observation, thus producing a partially hollow PS-rich core. In contrast, the high degree of grafting of the latexes synthesized with BPO stabilized the PS occlusions contained in the PB-rich phase, yielding "salami" like morphologies similar to those observed in HIPS, but in a nanometric scale.

4. Conclusions

Waterborne nanoparticles of PS containing B-based rubbers with different molecular microstructures and morphologies were synthesized by ME polymerization. The size of the initial ME droplets were affected by the rubber content and its molecular weight. Only in the experiment with small amounts of low molecular weight SBR (1% wbop), the droplets diameter were close to 100 nm and an almost complete droplet nucleation was observed with the water soluble initiator KPS. With increased rubber contents, droplet diameters were larger than 200 nm, and the use of water-soluble initiators (KPS or TBHP/AA) induced significant secondary nucleation. The oil-soluble BPO initiator induced droplet nucleation, and this produced acceptable N_p/N_d ratios. But high temperatures and high BPO concentrations were required, due to the low efficiency of oil-soluble initiators; and these promoted the formation of a lower molecular weight PS compared to that obtained with water-soluble initiators.

Grafting efficiencies and particle morphologies were affected by the chemical nature of the initiator and the molecular characteristics of the base rubber. For SBR concentrations <10% wbop, intraparticle phase separation was not appreciable. For SBR concentration 10% wbop, the particles exhibited a core–shell morphology. In the case of PB, more complex particle morphologies were observed, which were affected by the initiator type and the degree of grafting. KPS induced a low degree of grafting, and the rubber particles exhibited 3-phases: a PS-rich shell, an intermediate PB-rich phase, and a partially polymerized PS-rich core. In contrast, BPO induced a high degree of grafting that stabilized the occluded PS domains, and yielded nanometric-scale "salami" morphologies.

Acknowledgements

To CONICET, ANPCyT, Universidad Nacional del Litoral, and Secretary of University Policies of the Educational Ministry of Argentina, for their financial support. We also acknowledge Dr. Julia Yañez (TEM service, CCT-CONICET-Bahía Blanca, Argentina) for her help with the TEM observations; and M.C. Brandolini and J.L. Castañeda (INTEC) for their help with the SEC measurements.

References

[1] Martin MF, Viola, JP, Wuensch JR. Preparation, Properties and applications of high-impact polystyrene. In: Scheirs J, Priddy D, editors. Modern styrenic polymers: polystyrenes and styrenic copolymers. Wiley series in polymer science. John Wiley & Sons Ltd.: England; 2003, p 247–80. [chapter 12].
[2] Meira GR, Estenoz DA, Luciani CV. Continuous bulk process for the production of high-impact polystyrene: recent developments in modeling and control. Macromol React Eng 2007;1(1):25–39.
[3] Maul J, Frushour BG, Kontoff JR, Eichenauer H, Ott KH. Polystyrene and styrene copolymers. In: Ullmann's encyclopedia of industrial chemistry. Wiley-VCH Verlag GmbH & Co.; 2002.
[4] Priddy DB. Styrene plastics. In: Kirk-Othmer encyclopedia of chemical technology, vol.42. 4th ed. John Wiley & Sons Inc.; 1998. p. 1–40.
[5] Wei R, Luo Y, Li Z. Synthesis of structured nanoparticles of styrene/butadiene block copolymers via RAFT seeded emulsion polymerization. Polymer 2010;51(17):3879–86.
[6] Gao G, Zhou C, Yang H, Zhang H. Influence of core–shell rubber particles synthesized with different initiation systems on the impact toughness of modified polystyrene. J Appl Polym Sci 2007;103(2):738–44.
[7] Dai R, Gao G, Zhanga H. Different deformation mechanisms of two modified-polystyrene bimodal systems. Polym Int 2010;59(6):738–42.
[8] Lopez A, Degrandi-Contraires E, Canetta E, Creton C, Keddie JL, Asua JM. Waterborne polyurethane-acrylic hybrid nanoparticles by miniemulsion polymerization: applications in pressure-sensitive adhesives. Langmuir 2011, 27(7):3878-3888.
[9] Li M, Daniels ES, Dimonie V, Sudol ED, El-Aasser MS. Preparation of polyurethane/acrylic hybrid nanoparticles via a miniemulsion polymerization process. Macromolecules 2005;38(10):4183–92.
[10] Canetta E, Marchal J, Lei C-H, Deplace F, König AM, Creton C, et al. A comparison of tackified, miniemulsion core-shell acrylic latex films with corresponding particle-blend films: structure-property relationships. Langmuir 2009;25(18):11021–31.
[11] Goikoetxea M, Minari RJ, Beristain I, Paulis M, Barandiaran MJ, Asua JM. Polymerization kinetics and microstructure of waterborne acrylic/alkyd nanocomposites synthesized by miniemulsion. J Polym Sci Part A: Polym Chem 2009;47(19):4871–85.
[12] Jia G, Cai N, Xu Y, Liu C, Tan X. Miniemulsion polymerization of styrene with liquid polybutadiene as the sole Co-stabilizer. Eur Polym J 2007;43(10):4453–9.
[13] Jeong P, Dimonie VL, Daniels ES, El-Aasser MS. Hybrid composites latexes. ACS Symp Ser 2002;801:357–73.
[14] Aerdts A. Microestructure of styrene methyl methacrylate copolymers grafted onto polybutadiene seeds. In: Ph.D. thesis. Technische Univ. Eindhoven, Netherlands; 1993.
[15] Peng FM. Polybutadiene grafting and crosslinking in high-impact polystyrene bulk thermal process. J Appl Polym Sci 1990;40(7–8):1289–302.
[16] Yalkowsky SH, Banerjee S. Aqueous solubility, methods of estimation for organic compounds. New York: Marcel Dekker; 1992.
[17] González IM, Meira GR, Oliva HM. Synthesis of polystyrene with mixtures of mono- and bifunctional initiators. J Appl Polym Sci 1996;59(6):1015.
[18] Salazar A, Gugliotta LM, Vega JR, Meira GR. Molecular weight control in a starved emulsion polymerization of styrene. Ind Eng Chem Res 1998;37(9):3582–91.
[19] Autran C, de la Cal JC, Asua JM. Miniemulsion polymerization kinetics using oil-soluble initiator. Macromolecules 2007;40(17):6233–8.
[20] Clementi LA, Vega JR, Gugliotta LM. Particle size distribution of multimodal polymer dispersions by multiangle dynamic light

scattering. Solution of the inverse problem on the basis of a genetic algorithm. Part Part Syst Charact 2010;27(5–6):146–57.
[21] Leal GP, Asua JM. Evolution of the morphology of HIPS particles. Polymer 2009;50(1):68–76.
[22] Huang N-J, Sundberg DC. Fundamental studies of grafting reactions in free radical copolymerization. III. Grafting of styrene, acrylate, and methacrylate monomers onto cis-polybutadiene using benzoyl peroxide initiator in solution polymerization. J Polym Sci Part A: Polym Chem 1995;33(15):2571–86.
[23] Minari RJ, Goikoetxea M, Beristain I, Paulis M, Barandiaran MJ, Asua JM. Post-polymerization of waterborne alkyd/acrylics. effect on polymer architecture and particle morphology. Polymer 2009;50(25):5892–900.
[24] Moad G, Solomon DH, editors. The chemistry of free radical polymerization. Elsevier Science Ltd.; 1995, p. 26–7.
[25] Estenoz DA, Valdez E, Oliva HM, Meira GR. Bulk polymerization of styrene in presence of polybutadiene: calculation of molecular macrostructure. J Appl Polym Sci 1996;59(5):861–85.
[26] Minari RJ, Vega JR, Gonzáles-Sierra M, Meira GR, Gugliotta LM. Emulsion polymerization of styrene with iso-octyl-3-mercaptopropionate as chain transfer agent. J Appl Polym Sci 2008;109(6):3944–52.
[27] Tsavalas JG, Luo Y, Hudda L, Schork FJ. Limiting conversion phenomenon in hybrid miniemulsion polymerization. Polym React Eng 2003;11(3):277–304.